ward surface pressure contours are a necessary condition for vortex stability but not a sufficient one, whereas the flow features from Fig. 3 can provide both the necessary and sufficient conditions for vortex stability and breakdown.

By contrast, for $\alpha = 30$ deg, the solution did not converge even in 1000 computation cycles and cannot therefore be directly compared with the others. However, an examination of the results developed at the 1000th cycle is a useful exercise. For example, Fig. 4 shows the vortex interaction become totally disorganized on the leeward surface, and a significant drop of the spanwise upper surface pressure is noted in Fig. 5. These figures imply that the vortex breakdown effect becomes dominant over the entire wing. The flowfield unsteadiness was noted in that the crossflow patterns at each computation stage continued to change throughout the solution process; that is, a nonstationary flowfield was observed.

To validate the numerical simulation of vortex breakdown phenomenon by the TEAM code, the experimental results of a 60-deg, sharp-edge, uncambered delta wing by Wentz and Kohlman[7] were qualitatively compared. Their data showed the initiation of vortex breakdown to occur at the trailing edge by $\alpha = 15$ deg; the maximum lift by $\alpha = 30$ deg; and breakdown point moved into apex region by $\alpha = 32$ deg, consequently causing a decrease in lift. By comparison, for this cambered 60-deg delta wing, the TEAM code yields converged results even with a large region of reversed flow over the wing as α increases from 23 to 28 deg. Although the corresponding peak suction value at the examined crossflow planes are shown to be more positive, nevertheless, due to a larger vortex interaction with the leeward surface (see Fig. 5), the total lift continues to increase. In Ref. 5, the computed lift characteristics in this α range compare reasonably well with the experimental data for the F-106B configuration. As the region of reversed flow moves into the apex region by $\alpha = 30$ deg, the solution does not converge.

Summary

The three-dimensional vortex breakdown phenomenon over a F-106B configuration has been studied by examining a variety of on- and off-surface flow features from the TEAM code. Although the flow separation of this code is triggered by the numerical dissipation, and the computed flowfield may not represent the real vortex breakdown phenomenon adequately, nonetheless, the general trend of vortex breakdown effect on computed lift characteristics is similar to the wind tunnel results. Of the flowfield features examined, the crossflow contours of axial velocity and total pressure can provide both the necessary and sufficient conditions for vortex stability and breakdown.

Acknowledgment

This research work was supported by NASA Langley Research Center under Contract NAS1-17919, with John E. Lamar as the technical monitor.

References

[1]Hitzel, S. M. and Schmidt, W., "Slender Wings with Leading Edge Vortex Separation—A Challenge for Panel Methods and Euler Solvers," *Journal of Aircraft*, Vol. 21, Oct. 1984, pp. 751-759.

[2]Rizzi, A. and Purcell, C. J., "Disordered Vortex Flow Computed Around a Cranked Delta Wing and at Subsonic Speed and High Incidence," International Council of Aeronautical Sciences, Paper ICAS-86-1.4.1, Sept. 1986.

[3]Raj, P., Keen, J. M., and Singer, S. W., "Applications of an Euler Aerodynamic Method to Free-Vortex Flow Simulation," *Proceedings of the AIAA 6th Applied Aerodynamics Conference*, AIAA, New York, June 1988.

[4]Raj, P. and Brennan, J. "Improvements to an Euler Aerodynamic Method for Transonic Flow Analysis," AIAA Paper 87-0040, Jan. 1987.

[5]Pao, J. L., "Vortex Flow Analysis for F-106B Configuration," *Proceedings of the First National Fluid Dynamics Congress*, AIAA, Washington, DC, July 1988.

[6]Agarwal, R. K. and Deese, J. E. "Transonic Wing-Body Calculations Using Euler Equations," AIAA Paper 83-0501, Jan. 1983.

[7]Wentz, W. H. and Kohlman, D. L., "Vortex Breakdown On Slender Sharp-Edge Wings," AIAA Paper 69-778, July 1969.

Incompressible Viscous Flow About Aircraft Configurations

K. P. Sinhamahapatra,* N. Singh,† and B. C. Basu‡
Indian Institute of Technology, Kaharagpur, India

Nomenclature

A_{ik}, B_{ik} C_{ik}, D_{ik}	= normal components of velocities induced at the jth collocation point by the kth surface source, bound vorticity, line source, and horseshoe vortex respectively
$\mathcal{R}$	= aspect ratio
C_L	= total lift coefficient
C_l	= sectional lift coefficient
$C_{M_{LE}}$	= pitching-moment coefficient about wing leading edge
C_P	= pressure coefficient
c	= chord, m
D	= fuselage diameter (Fig. 2), m
h_1, h_2, g	= metrics of the nonorthogonal curvilinear coordinate system used in three-dimensional boundary-layer calculation
L_0	= fuselage length, m
N_T	= total number of singularities
$\hat{n}$	= outward unit normal vector
q	= function of metrics, $(q^2 = h_1^2 h_2^2 - g^2)$
R_N	= Reynolds number
s	= semispan, m
u_e	= resultant velocity at the edge of boundary layer
V	= total velocity vector
V_{ik}	= generalized induced velocity at the jth control point due to the kth generalized singularity
V_∞	= freestream velocity vector
W_{iw}	= transpiration velocity
α	= angle of attack
Γ	= strength of horseshoe vortex
γ	= vorticity strength
Δ_1, Δ_2	= displacement thicknesses in the nonorthogonal curvilinear coordinate system
δ_1, δ_2	= streamwise and cross-flow displacement thicknesses
ϵ	= wing setting angle
Π_k	= generalized singularity
σ	= source strength
Ω_{LE}	= leading-edge sweep back

Subscripts

t	= tail quantity
w	= wing quantiy

Received June 22, 1989; revision received July 31, 1989.

*Research Staff, Aeronautical Engineering Department.
†Assistant Professor, Aeronautical Engineering Department.
‡Professor, Aeronautical Engineering Department.

Introduction

A PROPER understanding and accurate calculation of the flowfield around complete aircraft is essential to provide aerodynamic data for the designer. Such data are generally obtained by finding inviscid solutions, although the viscous effect may be significant in many cases. In the viscous-inviscid interaction technique described by Lock and Williams,[1] mutual influence of the viscous and inviscid regions has been successfully applied to a number of practical flow problems by coupling the separate treatments of the two regions in such a way that their solutions match at some notional interface. Using this technique, an economical "viscous" panel method has been developed in this paper for the three-dimensional viscous flow over aircraft configurations.

In the present method, the inviscid flow is calculated by a panel method using the internal singularity distribution approach of Singh et al.[2] Such a flow model is likely to give an adequately accurate solution with a smaller number of panels because the distributed singularities placed inside the lifting surfaces induce smoother velocity variations on the wetted surfaces. The number of influence coefficients to be calculated in an internal singularity distribution method is considerably lower than that required for a surface singularity method. Since a major part of the numerical procedure is the calculation of influence coefficients, the total computing time and storage required for the solution of a given configuration is reduced considerably. The three-dimensonal boundary layers are calculated using an integral method, based on an entrainment principle, from Smith.[3] These calculation methods are coupled in an iterative scheme using a surface transpiration model to simulate the boundary-layer displacement effects. The predicted results are compared with experimental values.[4-6] The agreement appears to be most encouraging.

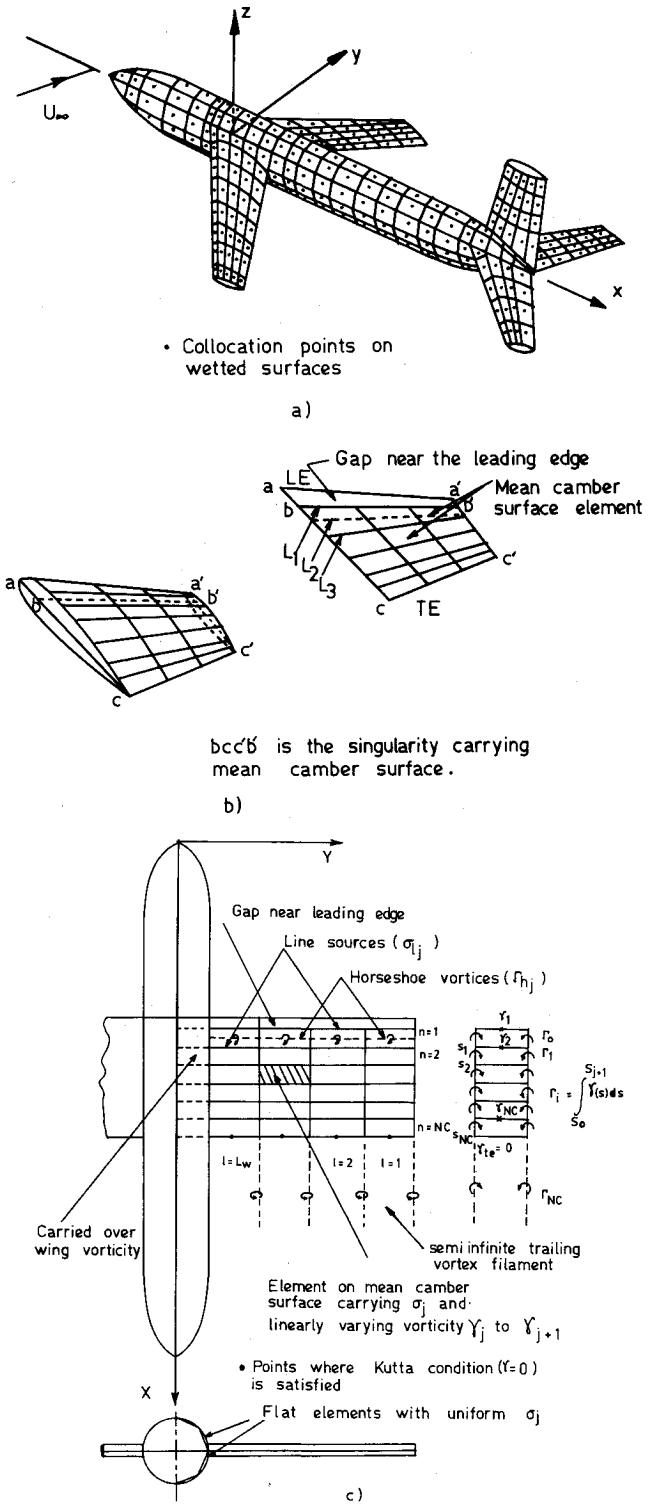

Fig. 1 a) Discretization of the configuration geometry used for the potential flow calculation, b) formation of a singularity carrying mean camber surface, and c) discretization of the singularity distribution used for the present potential flow calculation.

Present Numerical Approach

The external inviscid potential flow is calculated by a first-order panel method using an internal singularity distribution approach.[2] The method utilizes a distribution of source and vorticity singularities on the respective mean camber surfaces of wing and wing-like components. The fuselage carries only a source distribution on its wetted surface. The nonzero-bound vorticity strength at the wing-body junction has been carried over into the fuselage up to the midplane to model the interference effects at the junction to some extent. The same treatment is incorporated for the tail-plane-fuselage junction or tail-plane-fin junction. The unknown singularity strengths are solved by satisfying the boundary condition of prescribed normal velocity at the collocation points. The Kutta condition for this method simply states that the bound vorticity strength at the trailing edges of the lifting components are zero.

Discretization of the geometry and of the singularity carrying surfaces are shown in Fig. 1. This discretizaiton leads to a set of linear algebraic equations for the unknown singularity distribution which can be written as

$$\sum_{k=1}^{(I-1)(M-1)} A_{ik}\sigma_{sk} + \sum_{k=1}^{(I-1)(M-1)} B_{ik}\gamma_k + \sum_{k=1}^{M-1} C_{ik}(\sigma_{L_{1k}} + \sigma_{L_{2k}}) + \sum_{k=1}^{M-1} D_{ik}\Gamma_{hk} = -\hat{n}_i \cdot V_\infty$$

$$i = 1, 2, \ldots\ldots, 2(I-1)(M-1) \qquad (1)$$

Once the solution is obtained, total velocity at the ith control point can be found from the equation

$$V_i = \sum_{k=1}^{N_T} V_{ik}\Pi_k + V_\infty \qquad (2)$$

Calculation of pressure coefficients at the collocation points and overall forces is then straightforward.

The three-dimensional, turbulent boundary-layer development is calculated using the integral method from Smith.[3] The governing partial differential equations are solved using an explicit finite difference technique. The forward step size is controlled by the requirement that the downstream point lies within the domain of influence of the upstream point and its immediate neighbors. The axes system introduced is such that x and y axes form a nonorthogonal curvilinear mesh on the body surface, the z axis being normal to the body surface. Bicubic spline interpolation is used to calculate the metrics of the surface coordinate system and their derivatives from the known Cartesian coordinates of the surface.

The transpiration velocity (W_{iw}) is obtained by integrating the continuity equation and is given by

$$W_{iw} = \frac{1}{q}\left[\frac{\mathrm{d}}{\mathrm{d}x}(u_e\Delta_1 q/h_1) + \frac{\mathrm{d}}{\mathrm{d}y}(u_e\Delta_2 q/h_2)\right] \qquad (3)$$

Under relaxation in coupling the inviscid and boundary-layer calculation is used to achieve quick convergence. In all of the cases studied, a factor of one-third is found to be quite suitable. Final convergence is assessed by the change in sectional lift coefficients of the configuration in subsequent iterations. Computer codes in Fortran-77 are developed and run on a Horizon-III minicomputer. The source programs are available with the authors.

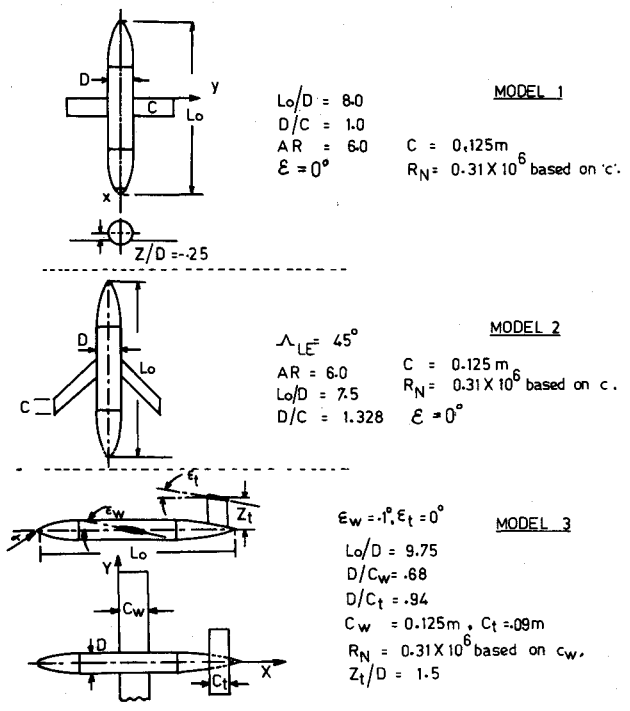

Fig. 2 Different test case models used for the present study; model 1—low rectangular wing-fuselage combination, model 2—swept wing-fuselage combination, model 3—wing-fuselage-tail-plane-fin combination.

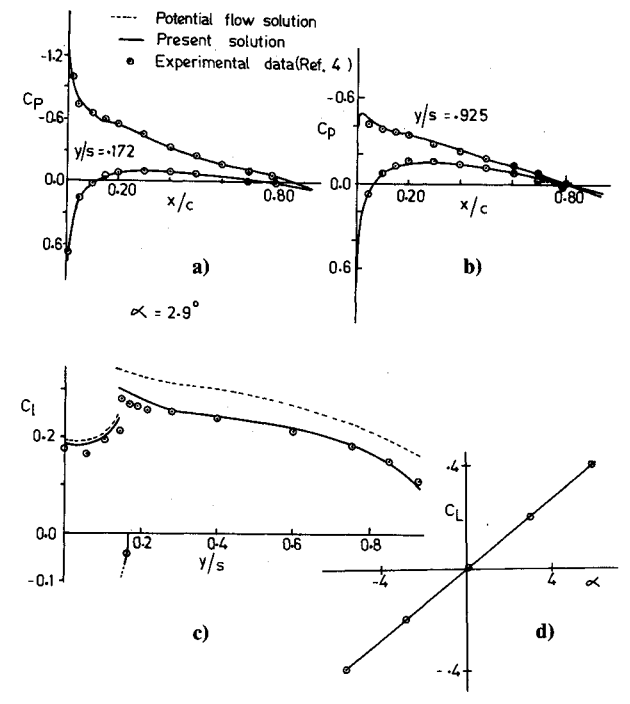

Fig. 3 Comparison of results for model 1; a) Pressure distribution on the wing at an angle of attack 2.9 deg at 17.2% semispan, b) pressure distribution on the wing at an angle of attack 2.9 deg at 92.5% semispan, c) lift distribution at 2.9-deg incidence, and d) variation of lift with angle of attack.

Discussion of Results

To illustrate the applicability of the present calculation method in wing-body or wing-body-tail-plane-fin interference studies, comparisons of measured and calculated pressure distributions are presented for the three case (models 1–3) shown in Fig. 2. In all of the cases, the wing has an aspect ratio of 6 and the airfoil section is 9%-thick RAE 101. The tail has an aspect ratio of 3 and a 12.6%-thick RAE 101 section. Comparison of variation of lift and pitching moment coefficients with angle of attack is also presented wherever experimental results are available.

Predicted numerical solutions for the low wing and fuselage combination are compared with the experimental values of Ref. 4 in Fig. 3. It is of interest to note that the present method is capable of obtaining all the finer details in both pressure and lift distribution. The variation of total lift with angle of attack is also shown in the figure. The overall agreement is most encouraging. Figure 4 presents comparison of predicted results with experimental values[5] for model 2. The correspondence shows a trend similar to the preceding case.

Results for a simple aircraft configuration consisting of wing, fuselage, tail plane, and fin are shown in Fig. 5. Experimental values are obtained from Ref. 6. Here also the calculated pressure and lift distributions predict all of the finer details observed in the trend of the experimental values. The variation of total lift and pitching moment about wing leading edge with angle of attack is also presented in the figure. The overall agreement of the predicted results with experimental data indicates that the present method is capable of giving satisfactory, accurate results for many engineering purposes.

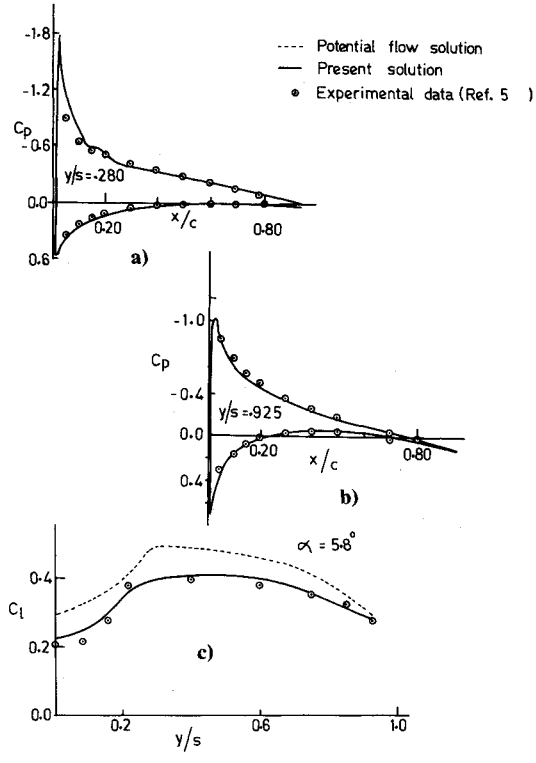

Fig. 4 Comparison of results for model 2; a) Pressure distribution on the wing at an angle of attack 5.8 deg at 28.0% semispan, b) pressure distribution on the wing at an angle of attack 5.8 deg at 92.5% semispan, and c) lift distribution at 5.8-deg incidence.

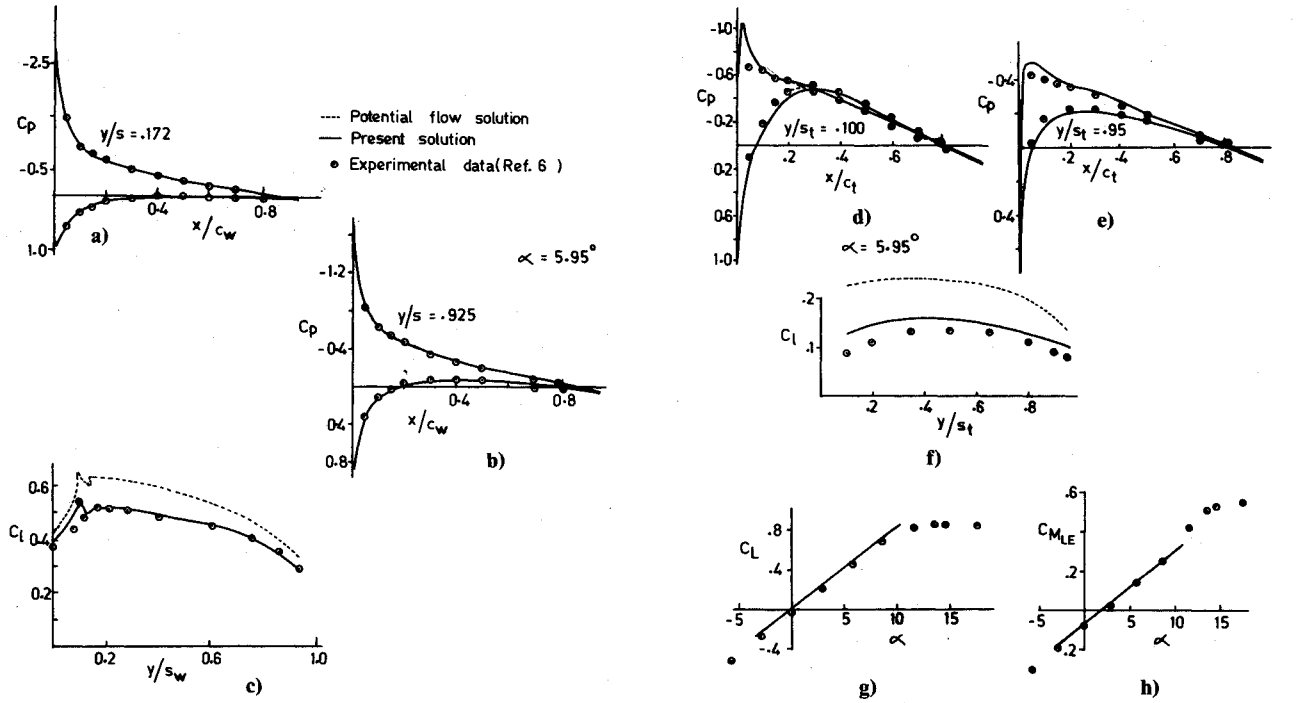

Fig. 5 Comparison of results for model 3; a) Pressure distribution on the wing at an angle of attack 5.95 deg at 17.2% semispan, b) pressure distribution on the wing at an angle of attack 5.95 deg at 92.5% semispan, c) wing-body lift distribution at 5.95-deg incidence, d) pressure distribution on the tail at 5.95-deg incidence at 10.0% tail semispan, e) pressure distribution on the tail at 5.95-deg incidence at 95.0% tail semispan, f) tail lift distribution at an angle of attack 5.95 deg, g) variation of lift with angle of attack h) variation of pitching moment about wing leading edge with angle of attack.

In order to reduce the number of plots in a figure for clarity, potential flow pressure distributions are not shown in the figures. However, the inviscid lift distribution curves are shown for all of the cases as representative solutions. It is observed that the potential flow solutions predict the trend fairly accurately, but the viscous effects are quite significant.

Conclusion

An economic viscous panel method capable of calculating the attached flow past aircraft configuration has been developed using an internal singularity distribution for the lifting components. The method gives satisfactory results with a number of panels significantly lower than a surface singularity method (the potential flow solution for the wing-fuselage-tail-plane-fin case is obtained with a total of 452 panels). Modeling of the interference effects in the junctions is quite rudimentary. However, the results obtained by the present method seem to be reasonably accurate for many engineering purposes.

Acknowledgment

The work was supported by the Aeronautical Research and Development Board, Ministry of Defence, India.

References

[1]Lock, R. C. and Williams, B. R., "Viscous-Inviscid Interactions in External Aerodynamics," *Progressive Aerospace Science,* Vol. 24, 1987, pp. 51-171.

[2]Singh, N., Bandyopadhyay, G., and Basu, B. C., "Calculation of Potential Flow about Arbitrary Three Dimensional Wings using Internal Singularity Distributions," *Aeronautical Quarterly,* Vol. 34, Aug. 1983, pp. 197-211.

[3]Smith, P. D., "An Integral Prediction Method for Three Dimensional Compressible Turbulent Boundary Layers," British Aeronautical Research Council, London, ARC R&M 3739, 1974.

[4]Korner, H., "Untersuchungen zur Bestimming der Druckverteilung an Flügel-Rumpf-Kombinationen," Vol. III, German Aerospace Research Establishment, Göttingen, FRG, DFVLR Berich 71/1, 1971.

[5]Korner, H., "Untersuchungen zur Bestimmung der Druckverteilung an Flügel-Rumpf-Kombinationen," Vol. II, German Aerospace Research Establishment, Göttingen, FRG, 1970.

[6]Korner, H. and Schroder, W., "Druckverteilungs und Kraftmessungen an einer Flügel-Rumpf-Leitwerk-Anordnung," German Aerospace Research Establishment, Göttingen, FRG, DFVLR IB 080-72/13, 1972.